

Radial Basis Functions collocation and a Unified Formulation for bending, vibration and buckling analysis of laminated plates, according to a variation of Murakami's zig-zag

*Original*

Radial Basis Functions collocation and a Unified Formulation for bending, vibration and buckling analysis of laminated plates, according to a variation of Murakami's zig-zag theory / Ferreira, A. J. M.; Roque, C. C.; Carrera, Erasmo; Cinefra, Maria; Polit, O.. - In: EUROPEAN JOURNAL OF MECHANICS. A, SOLIDS. - ISSN 0997-7538. - 30:4(2011), pp. 559-570. [10.1016/j.euromechsol.2011.01.007]

*Availability:*

This version is available at: 11583/2381109 since:

*Publisher:*

Elsevier

*Published*

DOI:10.1016/j.euromechsol.2011.01.007

*Terms of use:*

This article is made available under terms and conditions as specified in the corresponding bibliographic description in the repository

*Publisher copyright*

(Article begins on next page)

# Radial basis functions collocation and a unified formulation for bending, vibration and buckling analysis of laminated plates, according to a variation of Murakami's zig-zag theory

A.J.M. Ferreira <sup>a,\*</sup>, C.M.C. Roque <sup>b</sup>, E. Carrera <sup>c</sup>, M. Cinefra <sup>c</sup>, O. Polit <sup>d</sup>

<sup>a</sup> Departamento de Engenharia Mecânica, Faculdade de Engenharia da Universidade do Porto, Rua Dr. Roberto Frias, 4200-465 Porto, Portugal

<sup>b</sup> INEGI, Faculdade de Engenharia da Universidade do Porto, Rua Dr. Roberto Frias, 4200-465 Porto, Portugal

<sup>c</sup> Department of Aeronautics and Aerospace Engineering, Politecnico di Torino, Corso Duca degli Abruzzi, 24, 10129 Torino, Italy

<sup>d</sup> Université Paris Ouest e Nanterre, 50 rue de Sevres, 92410 Ville d'Avray, France

## 1. Introduction

The material properties of sandwich or layered composite laminates may present significant variations, which produce a discontinuity of the displacement at each layer interface, as seen in Fig. 1.

This is also known as zig-zag (ZZ) effect in laminated structures. An historical review on zig-zag theories has been provided by Carrera (2003).

Such discontinuities make difficult the use of classical theories such as Kirchhoff (1850) or Reissner (1945); Mindlin (1951) type theories (to trace accurate responses of sandwich structures, see the books by Zenkert (1995), and Vinson (1999)). The so called layerwise models in which the number of degrees-of-freedom increases with the increase in the number of layers, can be used to capture the above ZZ effect (see the overviews by Burton and Noor (1995), Noor et al. (1996), Altenbach (1998), Librescu and Hause (2000), Vinson (2001), and Demasi (2008a)). However, these models can be computational expensive, for laminates with large number of layers.

In the framework of mixed multi-layered plate theories, Murakami (1986) proposed a zig-zag function (ZZF) that is able to

reproduce the slope discontinuity for displacements. Equivalent single layer models with only displacement unknowns can be developed on the basis of ZZF, containing a zig-zag function that incorporates such discontinuity. A review of early developments in the application of ZZF has been provided in the review article by Carrera (2001). The advantages of using the ZZF to analyse multi-layered anisotropic plate and shells as well as the Finite Element implementation have been discussed by Carrera (2004).

In the present work the attention is restricted to the application of ZZF to bending, vibration and buckling analysis of laminated plates by collocation with radial basis functions. A new displacement theory is used, introducing a quadratic variation in  $z$  of the transverse displacements. This can be seen as a variation of the Murakami's ZZ displacement field (MZZF) (Murakami, 1986). Further studies on the use of MZZF have been documented in Carrera (2004), Demasi (2008b), Brischetto et al. (2009).

Recently, radial basis functions (RBFs) have enjoyed considerable success and research as a technique for interpolating data and functions. A radial basis function,  $\phi(\|x - x_j\|)$  is a spline that depends on the Euclidian  $n$ -dimensional distance between  $N$  distinct data centers  $x_j$ ,  $j = 1, 2, \dots, N \in \mathbb{R}^n$ , also called nodal or collocation points. Although most work to date on RBFs relates to scattered data approximation and in general to interpolation theory, there has recently been an increased interest in their use for solving partial

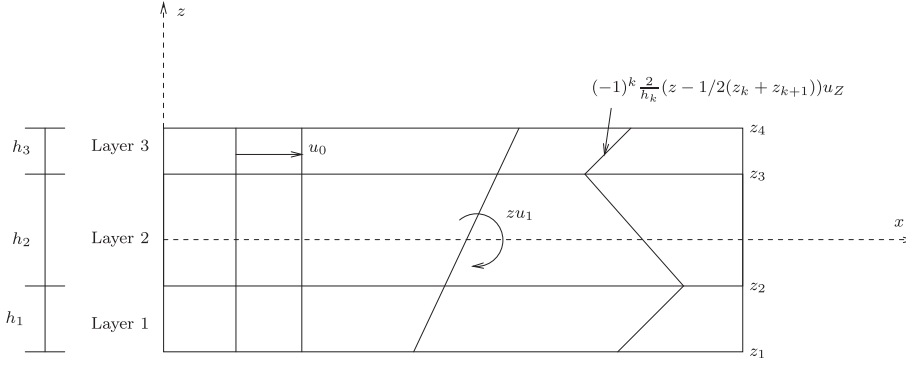


**Fig. 1.** Scheme of the zig-zag assumptions for a three-layered laminate: evolution of displacements in the thickness direction.

differential equations (PDEs). This approach, which approximates the whole solution of the PDE directly using RBFs, is truly a mesh-free technique. Kansa (1990) introduced the concept of solving PDEs by an unsymmetric RBF collocation method based upon the MQ interpolation functions, in which the shape parameter may vary across the problem domain. The use of alternative methods to the Finite Element Methods for the analysis of plates, such as the meshless methods based on radial basis functions, is attractive due to the absence of a mesh and the ease of collocation methods. The use of radial basis function for the analysis of structures and materials has been previously studied by numerous authors (Hon et al., 1997; Hon et al., 1999; Wang et al., 2002; Liu and Gu, 2001; Liu and Wang, 2002; Wang and Liu, 2002; Chen et al., 2003; Dai et al., 2004; Liu and Chen, 2002; Liew et al., 2004; Huang and Li, 2004; Liu et al., 2002; Xiang et al., 2009, 2010). A very interesting new technique that may provide excellent results for laminated plates in a near future was recently proposed by Liu et al. (Liu and Nguyen Thoi Trung, 2010; Liu et al., 2009; Nguyen-Xuan et al., 2009a, 2009b; Nguyen-Thoi et al., 2009, 2010). The authors have recently applied the RBF collocation to the static deformations of composite beams and plates (Ferreira, 2003a, 2003b; Ferreira et al., 2003). Although the present paper addresses linear problems only, extension to non-linear problems is possible as shown in works of Hon and colleagues (Wen and Hon, 2007).

In this paper it is investigated for the first time how the Unified Formulation can be combined with radial basis functions to the analysis of thick laminated plates, using a variation of the Murakami's zig-zag function, allowing for through-the-thickness deformations. Also, a new expansion of displacements is presented for the first time. This new approach represents a variation of the Murakami's original displacement field. The Unified Formulation gives a unified treatment to all variables (in this case, displacement field variables), allowing a systematic and fast derivation of equilibrium equation, regardless of number of degrees-of-freedom. The quality of the present method in predicting static deformations, free vibrations and buckling loads of thin and thick laminated plates is compared and discussed with other methods in some numerical examples.

## 2. The new zig-zag function

Let us consider a laminated plate composed of perfectly bonded layers, being  $z$  the thickness coordinate of the whole plate while  $z_k$  is the layer thickness coordinate.  $a$  and  $h$  are length and thickness of the square laminated plate, respectively. The adimensioned layer coordinate  $\zeta_k = (2z_k)/h_k$  is further introduced ( $h_k$  is the thickness of the  $k$ th layer). The Murakami's zig-zag function  $Z(z)$  was defined according to the following formula (Murakami, 1986)

$$Z(z) = (-1)^k \zeta_k \quad (1)$$

$Z(z)$  has the following properties:

- (1) It is a piece-wise linear function of layer coordinates  $z(k)$ ,
- (2)  $Z(z)$  has unit amplitude for the whole layers,
- (3) the slope  $Z'(z) = dZ/dz$  assumes opposite sign between two-adjacent layers. Its amplitude is layer thickness independent.

A possible first order shear deformation theory (FSDT) has been investigated by Carrera (2004) and Demasi (2008), ignoring the through-the-thickness deformations:

$$u = u_0 + zu_1 + (-1)^k \frac{2}{h_k} \left( z - \frac{1}{2}(z_k + z_{k+1}) \right) u_z \quad (2)$$

$$v = v_0 + zv_1 + (-1)^k \frac{2}{h_k} \left( z - \frac{1}{2}(z_k + z_{k+1}) \right) v_z \quad (3)$$

$$w = w_0 \quad (4)$$

The additional degrees-of-freedom  $u_z, v_z$  have a meaning of displacement, and its amplitude is layer independent.

A refinement of FSDT by inclusion of ZZ effects and transverse normal strains was introduced in Murakami's original ZZF, defined by the following displacement field:

$$u = u_0 + zu_1 + (-1)^k \frac{2}{h_k} \left( z - \frac{1}{2}(z_k + z_{k+1}) \right) u_z \quad (5)$$

$$v = v_0 + zv_1 + (-1)^k \frac{2}{h_k} \left( z - \frac{1}{2}(z_k + z_{k+1}) \right) v_z \quad (6)$$

$$w = w_0 + zw_1 + (-1)^k \frac{2}{h_k} \left( z - \frac{1}{2}(z_k + z_{k+1}) \right) w_z \quad (7)$$

The present ZZF theory involves the following (new) expansion of displacements

$$u = u_0 + zu_1 + (-1)^k \frac{2}{h_k} \left( z - \frac{1}{2}(z_k + z_{k+1}) \right) u_z \quad (8)$$

$$v = v_0 + zv_1 + (-1)^k \frac{2}{h_k} \left( z - \frac{1}{2}(z_k + z_{k+1}) \right) v_z \quad (9)$$

$$w = w_0 + zw_1 + z^2 w_2 \quad (10)$$

where  $z_k, z_{k+1}$  are the bottom and top  $z$ -coordinates at each layer. This represents a variation of the Murakami's original theory,

allowing for a quadratic evolution of the transverse displacement in the thickness direction.

### 3. The unified formulation

The Unified Formulation (UF) proposed by Carrera (2001, 1996, 1998), Carrera and Kroplin (1997), also known as CUF, is a powerful framework for the analysis of beams, plates and shells. This formulation has been applied in several finite element analyses, either using the Principle of Virtual Displacements, or by using the Reissner's Mixed Variational theorem. The stiffness matrix components, the external force terms or the inertia terms can be obtained directly with this UF, irrespective of the shear deformation theory being considered.

In this section the Carrera's Unified formulation (Carrera, 2001; Carrera, 1996; Carrera and Kroplin, 1997; Carrera, 1998) is briefly reviewed. It is shown how to obtain the fundamental nuclei, which allows the derivation of the equations of motion and boundary conditions, in weak form for the finite element analysis; and in strong form for the present RBF collocation.

#### 3.1. Governing equations and boundary conditions in the framework of unified formulation

Although one can use the UF for a one-layer, isotropic plate, a multi-layered plate with  $N_l$  layers is considered. The Principle of Virtual Displacements (PVD) for the pure-mechanical case reads:

$$\sum_{k=1}^{N_l} \int_{\Omega_k} \int_{A_k} \left\{ \delta \epsilon_{pG}^k T \sigma_{pC}^k + \delta \epsilon_{nG}^k T \sigma_{nC}^k \right\} d\Omega_k dz = \sum_{k=1}^{N_l} \delta L_e^k \quad (11)$$

where  $\Omega_k$  and  $A_k$  are the integration domains in plane ( $x, y$ ) and  $z$  direction, respectively. Here,  $k$  indicates the layer and  $T$  the transpose of a vector, and  $\delta L_e^k$  is the external virtual work for the  $k$ th layer.  $G$  means geometrical relations and  $C$  constitutive equations.

The steps to obtain the governing equations are:

- Substitution of the geometrical relations (subscript G)
- Substitution of the appropriate constitutive equations (subscript C)
- Introduction of the Unified Formulation

Stresses and strains are separated into in-plane and through-the-thickness components, denoted respectively by the subscripts  $p$  and  $n$ . The mechanical strains in the  $k$ th layer can be related to the displacement field  $\mathbf{u}^k = \{u_x^k, u_y^k, u_z^k\}$  via the geometrical relations:

$$\begin{aligned} \epsilon_{pG}^k &= [\epsilon_{xx}, \epsilon_{yy}, \gamma_{xy}]^{kT} = \mathbf{D}_p^k \mathbf{u}^k, \\ \epsilon_{nG}^k &= [\gamma_{xz}, \gamma_{yz}, \epsilon_{zz}]^{kT} = (\mathbf{D}_{np}^k + \mathbf{D}_{nz}^k) \mathbf{u}^k, \end{aligned} \quad (12)$$

wherein the differential operator arrays are defined as follows:

$$\mathbf{D}_p^k = \begin{bmatrix} \partial_x & 0 & 0 \\ 0 & \partial_y & 0 \\ \partial_y & \partial_x & 0 \end{bmatrix}, \mathbf{D}_{np}^k = \begin{bmatrix} 0 & 0 & \partial_x \\ 0 & 0 & \partial_y \\ 0 & 0 & 0 \end{bmatrix}, \mathbf{D}_{nz}^k = \begin{bmatrix} \partial_z & 0 & 0 \\ 0 & \partial_z & 0 \\ 0 & 0 & \partial_z \end{bmatrix}, \quad (13)$$

The 3D constitutive equations are given as:

$$\begin{aligned} \sigma_{pC}^k &= \mathbf{C}_{pp}^k \epsilon_{pG}^k + \mathbf{C}_{pn}^k \epsilon_{nG}^k \\ \sigma_{nC}^k &= \mathbf{C}_{np}^k \epsilon_{pG}^k + \mathbf{C}_{nn}^k \epsilon_{nG}^k \end{aligned} \quad (14)$$

with

$$\begin{aligned} \mathbf{C}_{pp}^k &= \begin{bmatrix} C_{11} & C_{12} & C_{16} \\ C_{12} & C_{22} & C_{26} \\ C_{16} & C_{26} & C_{66} \end{bmatrix}, \mathbf{C}_{pn}^k = \begin{bmatrix} 0 & 0 & C_{13} \\ 0 & 0 & C_{23} \\ 0 & 0 & C_{36} \end{bmatrix} \\ \mathbf{C}_{np}^k &= \begin{bmatrix} 0 & 0 & 0 \\ 0 & 0 & 0 \\ C_{13} & C_{23} & C_{36} \end{bmatrix}, \mathbf{C}_{nn}^k = \begin{bmatrix} C_{55} & C_{45} & 0 \\ C_{45} & C_{44} & 0 \\ 0 & 0 & C_{33} \end{bmatrix} \end{aligned} \quad (15)$$

According to the Unified Formulation by Carrera, the three displacement components  $u_x, u_y$  and  $u_z$  and their relative variations can be modelled as:

$$\begin{aligned} (u_x, u_y, u_z) &= F_\tau (u_{x\tau}, u_{y\tau}, u_{z\tau}) \quad (\delta u_x, \delta u_y, \delta u_z) \\ &= F_s (\delta u_{xs}, \delta u_{ys}, \delta u_{zs}) \end{aligned} \quad (16)$$

with Taylor expansions from first up to 4th order:  $F_0 = z^0 = 1$ ,  $F_1 = z^1 = z$ , ...,  $F_N = z^N$ , ...,  $F_4 = z^4$  if an Equivalent Single Layer (ESL) approach is used.

In Fig. 2 it is shown the assembling procedures on layer  $k$  for ESL approach. It is shown that after the computation of the contribution of individual layers the assembly process is linked to the same degrees-of-freedom. A different approach is performed in layerwise theories, where the assembly process is linked to degrees-of-freedom that are connected to individual layers (see Carrera (2004) for more detail). Substituting the geometrical relations, the constitutive equations and the unified formulation into the variational statement PVD, for the  $k$ th layer, one has:

$$\begin{aligned} \int_{\Omega_k} \int_{A_k} \left[ \left( \mathbf{D}_p^k F_s \delta \mathbf{u}_s^k \right)^T \left( \mathbf{C}_{pp}^k \mathbf{D}_p^k F_\tau \mathbf{u}_\tau^k + \mathbf{C}_{pn}^k \left( \mathbf{D}_{n\Omega}^k + \mathbf{D}_{nz}^k \right) F_\tau \mathbf{u}_\tau^k \right) \right. \\ \left. + \left( \left( \mathbf{D}_{n\Omega}^k + \mathbf{D}_{nz}^k \right) F_s \delta \mathbf{u}_s^k \right)^T \left( \mathbf{C}_{np}^k \mathbf{D}_p^k F_\tau \mathbf{u}_\tau^k + \mathbf{C}_{nn}^k \left( \mathbf{D}_{n\Omega}^k + \mathbf{D}_{nz}^k \right) F_\tau \mathbf{u}_\tau^k \right) \right] \\ \times d\Omega_k dz = \delta L_e^k \end{aligned} \quad (17)$$

At this point, the formula of integration by parts is applied:

$$\begin{aligned} \int_{\Omega_k} \left( (\mathbf{D}_\Omega) \delta \mathbf{a}^k \right)^T \mathbf{a}^k d\Omega_k &= - \int_{\Omega_k} \delta \mathbf{a}^{kT} \left( (\mathbf{D}_\Omega^T) \mathbf{a}^k \right) d\Omega_k \\ &+ \int_{\Gamma_k} \delta \mathbf{a}^{kT} \left( (\mathbf{I}_\Omega) \mathbf{a}^k \right) d\Gamma_k \end{aligned} \quad (18)$$

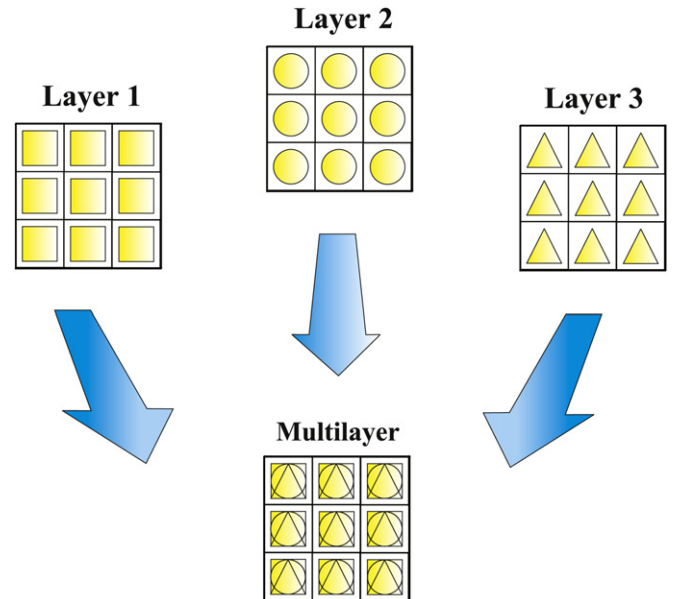


Fig. 2. Assembling procedure for ESL approach.

where the  $\mathbf{I}_\Omega$  matrix is obtained applying the *Divergence theorem*:

$$\int_{\Omega} \frac{\partial \psi}{\partial x_i} dv = \oint_{\Gamma} n_i \psi ds \quad (19)$$

In (19)  $n_i$  are the components of the normal  $\hat{n}$  to the boundary along the direction  $i$ . After integration by parts, the governing equations and boundary conditions for the plate in the mechanical case are obtained:

$$\begin{aligned} & \int_{\Omega_k} \int_{A_k} (\delta \mathbf{u}_s^k)^T \left[ \left( (-\mathbf{D}_p^k)^T (\mathbf{C}_{pp}^k (\mathbf{D}_p^k) + \mathbf{C}_{pn}^k (\mathbf{D}_{n\Omega}^k + \mathbf{D}_{nz}^k)) \right. \right. \\ & \quad \left. \left. + (-\mathbf{D}_{n\Omega}^k + \mathbf{D}_{nz}^k)^T (\mathbf{C}_{np}^k (\mathbf{D}_p^k) + \mathbf{C}_{nn}^k (\mathbf{D}_{n\Omega}^k + \mathbf{D}_{nz}^k)) \right) \right. \\ & \quad \left. \times \mathbf{F}_\tau \mathbf{F}_s \mathbf{u}_\tau^k \right] dx dy dz + \int_{\Omega_k} \int_{A_k} (\delta \mathbf{u}_s^k)^T \left[ \left( \mathbf{I}_p^{kT} (\mathbf{C}_{pp}^k (\mathbf{D}_p^k) \right. \right. \\ & \quad \left. \left. + \mathbf{C}_{pn}^k (\mathbf{D}_{n\Omega}^k + \mathbf{D}_{nz}^k)) \right) \right. \\ & \quad \left. + \mathbf{I}_{np}^{kT} (\mathbf{C}_{np}^k (\mathbf{D}_p^k) + \mathbf{C}_{nn}^k (\mathbf{D}_{n\Omega}^k + \mathbf{D}_{nz}^k)) \mathbf{F}_\tau \mathbf{F}_s \mathbf{u}_\tau^k \right] dx dy dz \\ & = \int_{\Omega_k} \delta \mathbf{u}_s^{kT} \mathbf{F}_s \mathbf{p}_u^k d\Omega_k. \end{aligned} \quad (20)$$

where  $\mathbf{I}_p^k$  and  $\mathbf{I}_{np}^k$  depend on the boundary geometry:

$$\mathbf{I}_p^k = \begin{bmatrix} n_x & 0 & 0 \\ 0 & n_y & 0 \\ n_y & n_x & 0 \end{bmatrix}, \mathbf{I}_{np}^k = \begin{bmatrix} 0 & 0 & n_x \\ 0 & 0 & n_y \\ 0 & 0 & 0 \end{bmatrix}. \quad (21)$$

The normal to the boundary of domain  $\Omega$  is:

$$\hat{n} = \begin{bmatrix} n_x \\ n_y \end{bmatrix} = \begin{bmatrix} \cos(\varphi_x) \\ \cos(\varphi_y) \end{bmatrix} \quad (22)$$

where  $\varphi_x$  and  $\varphi_y$  are the angles between the normal  $\hat{n}$  and the direction  $x$  and  $y$  respectively.

The governing equations for a multi-layered plate subjected to mechanical loadings are:

$$\delta \mathbf{u}_s^{kT} : \mathbf{K}_{uu}^{kts} \mathbf{u}_\tau^k = \mathbf{P}_{u\tau}^k \quad (23)$$

where the fundamental nucleus  $\mathbf{K}_{uu}^{kts}$  is obtained as:

$$\begin{aligned} \mathbf{K}_{uu}^{kts} = & \left[ (-\mathbf{D}_p^k)^T \mathbf{C}_{pp}^k (\mathbf{D}_p^k) + \mathbf{C}_{pn}^k (\mathbf{D}_{n\Omega}^k + \mathbf{D}_{nz}^k) + (-\mathbf{D}_{n\Omega}^k \right. \\ & \left. + \mathbf{D}_{nz}^k)^T (\mathbf{C}_{np}^k (\mathbf{D}_p^k) + \mathbf{C}_{nn}^k (\mathbf{D}_{n\Omega}^k + \mathbf{D}_{nz}^k)) \right] \mathbf{F}_\tau \mathbf{F}_s \end{aligned} \quad (24)$$

and the corresponding Neumann-type boundary conditions on  $\Gamma_k$  are:

$$\mathbf{\Pi}_d^{kts} \mathbf{u}_\tau^k = \mathbf{\Pi}_d^{kts} \bar{\mathbf{u}}_\tau^k, \quad (25)$$

where:

$$\begin{aligned} \mathbf{\Pi}_d^{kts} = & \left[ \mathbf{I}_p^{kT} (\mathbf{C}_{pp}^k (\mathbf{D}_p^k) + \mathbf{C}_{pn}^k (\mathbf{D}_{n\Omega}^k + \mathbf{D}_{nz}^k)) + \mathbf{I}_{np}^{kT} (\mathbf{C}_{np}^k (\mathbf{D}_p^k) \right. \\ & \left. + \mathbf{C}_{nn}^k (\mathbf{D}_{n\Omega}^k + \mathbf{D}_{nz}^k)) \right] \mathbf{F}_\tau \mathbf{F}_s \end{aligned} \quad (26)$$

and  $\mathbf{P}_{u\tau}^k$  are variationally consistent loads with applied pressure.

### 3.2. Fundamental nuclei

The fundamental nuclei in explicit form are then obtained as:

$$\begin{aligned} K_{uu11}^{kts} &= \left( -\partial_x^\tau \partial_x^s C_{11} - \partial_x^\tau \partial_y^s C_{16} + \partial_z^\tau \partial_z^s C_{55} - \partial_y^\tau \partial_x^s C_{16} - \partial_y^\tau \partial_y^s C_{66} \right) F_\tau F_s \\ K_{uu12}^{kts} &= \left( -\partial_x^\tau \partial_y^s C_{12} - \partial_x^\tau \partial_x^s C_{16} + \partial_z^\tau \partial_z^s C_{45} - \partial_y^\tau \partial_y^s C_{26} - \partial_y^\tau \partial_x^s C_{66} \right) F_\tau F_s \\ K_{uu13}^{kts} &= \left( -\partial_x^\tau \partial_z^s C_{13} - \partial_y^\tau \partial_z^s C_{36} + \partial_z^\tau \partial_y^s C_{45} + \partial_z^\tau \partial_x^s C_{55} \right) F_\tau F_s \\ K_{uu21}^{kts} &= \left( -\partial_y^\tau \partial_x^s C_{12} - \partial_y^\tau \partial_y^s C_{26} + \partial_z^\tau \partial_z^s C_{45} - \partial_x^\tau \partial_x^s C_{16} - \partial_x^\tau \partial_y^s C_{66} \right) F_\tau F_s \\ K_{uu22}^{kts} &= \left( -\partial_y^\tau \partial_y^s C_{22} - \partial_y^\tau \partial_x^s C_{26} + \partial_z^\tau \partial_z^s C_{44} - \partial_x^\tau \partial_y^s C_{26} - \partial_x^\tau \partial_x^s C_{66} \right) F_\tau F_s \\ K_{uu23}^{kts} &= \left( -\partial_y^\tau \partial_z^s C_{23} - \partial_x^\tau \partial_z^s C_{36} + \partial_z^\tau \partial_y^s C_{44} + \partial_z^\tau \partial_x^s C_{45} \right) F_\tau F_s \\ K_{uu31}^{kts} &= \left( \partial_z^\tau \partial_x^s C_{13} + \partial_z^\tau \partial_y^s C_{36} - \partial_y^\tau \partial_z^s C_{45} - \partial_x^\tau \partial_z^s C_{55} \right) F_\tau F_s \\ K_{uu32}^{kts} &= \left( \partial_z^\tau \partial_y^s C_{23} + \partial_z^\tau \partial_x^s C_{36} - \partial_y^\tau \partial_z^s C_{44} - \partial_x^\tau \partial_z^s C_{45} \right) F_\tau F_s \\ K_{uu33}^{kts} &= \left( \partial_z^\tau \partial_z^s C_{33} - \partial_y^\tau \partial_y^s C_{44} - \partial_y^\tau \partial_x^s C_{45} - \partial_x^\tau \partial_y^s C_{45} - \partial_x^\tau \partial_x^s C_{55} \right) F_\tau F_s \end{aligned} \quad (27)$$

$$\begin{aligned} \Pi_{11}^{kts} &= \left( n_x \partial_x^s C_{11} + n_x \partial_y^s C_{16} + n_y \partial_x^s C_{16} + n_y \partial_y^s C_{66} \right) F_\tau F_s \\ \Pi_{12}^{kts} &= \left( n_x \partial_y^s C_{12} + n_x \partial_x^s C_{16} + n_y \partial_y^s C_{26} + n_y \partial_x^s C_{66} \right) F_\tau F_s \\ \Pi_{13}^{kts} &= \left( n_x \partial_z^s C_{13} + n_y \partial_z^s C_{36} \right) F_\tau F_s \\ \Pi_{21}^{kts} &= \left( n_y \partial_x^s C_{12} + n_y \partial_y^s C_{26} + n_x \partial_x^s C_{16} + n_x \partial_y^s C_{66} \right) F_\tau F_s \\ \Pi_{22}^{kts} &= \left( n_y \partial_y^s C_{22} + n_y \partial_x^s C_{26} + n_x \partial_y^s C_{26} + n_x \partial_x^s C_{66} \right) F_\tau F_s \\ \Pi_{23}^{kts} &= \left( n_y \partial_z^s C_{23} + n_x \partial_z^s C_{36} \right) F_\tau F_s \\ \Pi_{31}^{kts} &= \left( n_y \partial_z^s C_{45} + n_x \partial_z^s C_{55} \right) F_\tau F_s \\ \Pi_{32}^{kts} &= \left( n_y \partial_z^s C_{44} + n_x \partial_z^s C_{45} \right) F_\tau F_s \\ \Pi_{33}^{kts} &= \left( n_y \partial_y^s C_{44} + n_y \partial_x^s C_{45} + n_x \partial_y^s C_{45} + n_x \partial_x^s C_{55} \right) F_\tau F_s \end{aligned} \quad (28)$$

### 3.3. Dynamic governing equations

The PVD for the dynamic case is expressed as:

$$\begin{aligned} & \sum_{k=1}^{N_l} \int_{\Omega_k} \int_{A_k} \left\{ \delta \epsilon_{pG}^k T \sigma_{pC}^k + \delta \epsilon_{nG}^k T \sigma_{nC}^k \right\} d\Omega_k dz \\ & = \sum_{k=1}^{N_l} \int_{\Omega_k} \int_{A_k} \rho^k \delta \mathbf{u}^{kT} \ddot{\mathbf{u}}^k d\Omega_k dz + \sum_{k=1}^{N_l} \delta L_e^k \end{aligned} \quad (29)$$

where  $\rho^k$  is the mass density of the  $k$  th layer and double dots denote acceleration.

By substituting the geometrical relations, the constitutive equations and the Unified Formulation, we obtain the following governing equations:

$$\delta \mathbf{u}_s^{kT} : \mathbf{K}_{uu}^{kts} \mathbf{u}_\tau^k = -\mathbf{M}^{kts} \ddot{\mathbf{u}}_\tau^k + \mathbf{P}_{u\tau}^k \quad (30)$$

In the case of free vibrations one has:

$$\delta \mathbf{u}_s^{kT} : \mathbf{K}_{uu}^{kts} \mathbf{u}_\tau^k = -\mathbf{M}^{kts} \ddot{\mathbf{u}}_\tau^k \quad (31)$$

where  $\mathbf{M}^{kts}$  is the fundamental nucleus for the inertial term. The explicit form of that is:

$$M_{11}^{kts} = \rho^k F_\tau F_s; \quad M_{12}^{kts} = 0; \quad M_{13}^{kts} = 0 \quad (32)$$

$$M_{21}^{kts} = 0; \quad M_{22}^{kts} = \rho^k F_\tau F_s; \quad M_{23}^{kts} = 0 \quad (33)$$

$$M_{31}^{kts} = 0; \quad M_{32}^{kts} = 0; \quad M_{33}^{kts} = \rho^k F_\tau F_s \quad (34)$$

The geometrical and mechanical boundary conditions are the same of the static case.

Resorting to the displacement field in Eq. (18), we choose vectors  $F_t = [1z(-1)^k/2h_k(z - 1/2(z_k + z_{k+1}))]$  for displacements  $u, v$ , and  $F_t = [1 \quad z \quad z^2]$  for displacement  $w$ . We then obtain all terms of the equations of motion by integrating through-the-thickness direction.

It is interesting to note that under this combination of the Unified Formulation and RBF collocation, the collocation code depends only on the choice of  $F_t, F_s$ , in order to solve this type of problems. We designed a MATLAB code that just by changing  $F_t, F_s$  can analyse static deformations, free vibrations and buckling loads for any type of  $C^\infty$  shear deformation theory. An obvious advantage of the present methodology is that the tedious derivation of the equations of motion and boundary conditions for a particular shear deformation theory is no longer an issue.

#### 4. The radial basis function method

##### 4.1. The static problem

Radial basis functions (RBF) approximations are mesh-free numerical schemes that can exploit accurate representations of the boundary, are easy to implement and can be spectrally accurate. In this section the formulation of a global unsymmetrical collocation RBF-based method to compute elliptic operators is presented.

Consider a linear elliptic partial differential operator  $L$  and a bounded region  $\Omega$  in  $\mathbb{R}^n$  with some boundary  $\partial\Omega$ . In the static problems we seek the computation of displacements ( $\mathbf{u}$ ) from the global system of equations

$$\mathcal{L}\mathbf{u} = \mathbf{f} \text{ in } \Omega \quad (35)$$

$$\mathcal{L}_B\mathbf{u} = \mathbf{g} \text{ on } \partial\Omega \quad (36)$$

where  $\mathcal{L}, \mathcal{L}_B$  are linear operators in the domain and on the boundary, respectively. The right-hand side of (35) and (36) represent the external forces applied on the plate and the boundary conditions applied along the perimeter of the plate, respectively. The PDE problem defined in (35) and (36) will be replaced by a finite problem, defined by an algebraic system of equations, after the radial basis expansions.

##### 4.2. The eigenproblem

The eigenproblem looks for eigenvalues ( $\lambda$ ) and eigenvectors ( $\mathbf{u}$ ) that satisfy

$$\mathcal{L}\mathbf{u} + \lambda\mathbf{u} = 0 \text{ in } \Omega \quad (37)$$

$$\mathcal{L}_B\mathbf{u} = 0 \text{ on } \partial\Omega \quad (38)$$

As in the static problem, the eigenproblem defined in (37) and (38) is replaced by a finite-dimensional eigenvalue problem, based on RBF approximations.

##### 4.3. Radial basis functions approximations

The radial basis function ( $\phi$ ) approximation of a function ( $\mathbf{u}$ ) is given by

$$\tilde{\mathbf{u}}(\mathbf{x}) = \sum_{i=1}^N \alpha_i \phi(\|\mathbf{x} - \mathbf{y}_i\|_2), \mathbf{x} \in \mathbb{R}^n \quad (39)$$

where  $\mathbf{y}_i, i = 1, \dots, N$  is a finite set of distinct points (centers) in  $\mathbb{R}^n$ . The most common RBFs are

$$\text{Cubic: } \phi(r) = r^3$$

$$\text{Thin plate splines: } \phi(r) = r^2 \log(r)$$

$$\text{Wendland functions: } \phi(r) = (1 - r)^m p(r)$$

$$\text{Gaussian: } \phi(r) = e^{-(cr)^2}$$

$$\text{Multiquadrics: } \phi(r) = \sqrt{c^2 + r^2}$$

$$\text{Inverse Multiquadrics: } \phi(r) = (c^2 + r^2)^{-1/2}$$

where the Euclidian distance  $r$  is real and non-negative and  $c$  is a positive shape parameter. Hardy (1971) introduced multiquadrics in the analysis of scattered geographical data. In the 1990's Kansa (1990) used multiquadrics for the solution of partial differential equations. Considering  $N$  distinct interpolations, and knowing  $u(\mathbf{x}_j), j = 1, 2, \dots, N$ , we find  $\alpha_i$  by the solution of a  $N \times N$  linear system

$$\mathbf{A}\boldsymbol{\alpha} = \mathbf{u} \quad (40)$$

where  $\mathbf{A} = [\phi(\|\mathbf{x} - \mathbf{y}_i\|_2)]_{N \times N}$ ,  $\boldsymbol{\alpha} = [\alpha_1, \alpha_2, \dots, \alpha_N]^T$  and  $\mathbf{u} = [u(\mathbf{x}_1), u(\mathbf{x}_2), \dots, u(\mathbf{x}_N)]^T$ .

Since radial basis functions depend only on grid points and not on a mesh (in a finite element method sense), these can be irregularly distributed over the domain and boundaries. This is particularly important for problems with an irregular and complex geometry, as is often the case in engineering problems.

##### 4.4. Solution of the static problem

The solution of a static problem by radial basis functions considers  $N_I$  nodes in the domain and  $N_B$  nodes on the boundary, with a total number of nodes  $N = N_I + N_B$ . We denote the sampling points by  $\mathbf{x}_i \in \Omega, i = 1, \dots, N_I$  and  $\mathbf{x}_i \in \partial\Omega, i = N_I + 1, \dots, N$ . At the points in the domain we solve the following system of equations

$$\sum_{i=1}^N \alpha_i \mathcal{L}\phi(\|\mathbf{x} - \mathbf{y}_i\|_2) = \mathbf{f}(\mathbf{x}_j), j = 1, 2, \dots, N_I \quad (41)$$

or

$$\mathcal{L}^I \boldsymbol{\alpha} = \mathbf{F} \quad (42)$$

where

$$\mathcal{L}^I = [\mathcal{L}\phi(\|\mathbf{x} - \mathbf{y}_i\|_2)]_{N_I \times N} \quad (43)$$

At the points on the boundary, we impose boundary conditions as

$$\sum_{i=1}^N \alpha_i \mathcal{L}_B\phi(\|\mathbf{x} - \mathbf{y}_i\|_2) = \mathbf{g}(\mathbf{x}_j), j = N_I + 1, \dots, N \quad (44)$$

or

$$\mathbf{B}\boldsymbol{\alpha} = \mathbf{G} \quad (45)$$

where

$$\mathbf{B} = \mathcal{L}_B\phi(\|\mathbf{x}_{N_I+1} - \mathbf{y}_j\|_2)_{N_B \times N}$$

Therefore, we can write a finite-dimensional static problem as

$$\begin{bmatrix} \mathcal{L}^I \\ \mathbf{B} \end{bmatrix} \boldsymbol{\alpha} = \begin{bmatrix} \mathbf{F} \\ \mathbf{G} \end{bmatrix} \quad (46)$$

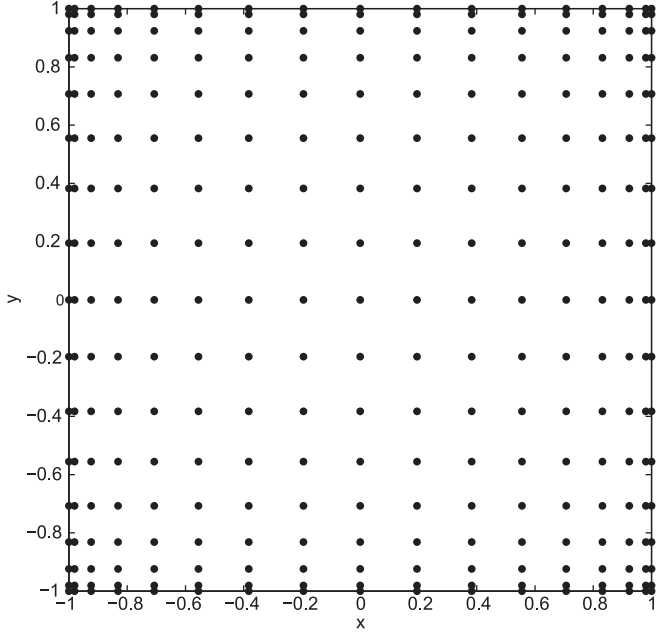


Fig. 3. Chebyshev grid.

By inverting the system (46), we obtain the vector  $\alpha$ . We then obtain the solution  $\mathbf{u}$  using the interpolation Eq. (39).

#### 4.5. Solution of the eigenproblem

We consider  $N_I$  nodes in the interior of the domain and  $N_B$  nodes on the boundary, with  $N = N_I + N_B$ . We denote interpolation points by  $x_i \in \Omega, i = 1, \dots, N_I$  and  $x_i \in \partial\Omega, i = N_I + 1, \dots, N$ . At the points in the domain, we define the eigenproblem as

$$\sum_{i=1}^N \alpha_i \mathcal{L} \phi(\|x - y_i\|_2) = \lambda \tilde{\mathbf{u}}(x_j), j = 1, 2, \dots, N_I \quad (47)$$

or

$$\mathcal{L}^I \alpha = \lambda \tilde{\mathbf{u}}^I \quad (48)$$

where

$$\mathcal{L}^I = [\mathcal{L} \phi(\|x - y_i\|_2)]_{N_I \times N} \quad (49)$$

At the points on the boundary, we enforce the boundary conditions as

$$\sum_{i=1}^N \alpha_i \mathcal{L} \phi(\|x - y_i\|_2) = 0, j = N_I + 1, \dots, N \quad (50)$$

or

$$\mathbf{B} \alpha = 0 \quad (51)$$

Eqs. (48) and (51) can now be solved as a generalized eigenvalue problem

$$\begin{bmatrix} \mathcal{L}^I \\ \mathbf{B} \end{bmatrix} \alpha = \lambda \begin{bmatrix} \mathbf{A}^I \\ 0 \end{bmatrix} \alpha \quad (52)$$

where

$$\mathbf{A}^I = \phi(\|x_{N_I} - y_j\|_2)_{N_I \times N}$$

#### 4.6. Discretization of the equations of motion and boundary conditions

The radial basis collocation method follows a simple implementation procedure. Taking Eq. (11), we compute

$$\alpha = \begin{bmatrix} \mathbf{L}^I \\ \mathbf{B} \end{bmatrix}^{-1} \begin{bmatrix} \mathbf{F} \\ \mathbf{G} \end{bmatrix} \quad (53)$$

This  $\alpha$  vector is then used to obtain solution  $\tilde{\mathbf{u}}$ , by using (6). If derivatives of  $\tilde{\mathbf{u}}$  are needed, such derivatives are computed as

$$\frac{\partial \tilde{\mathbf{u}}}{\partial x} = \sum_{j=1}^N \alpha_j \frac{\partial \phi_j}{\partial x} \quad (54)$$

$$\frac{\partial^2 \tilde{\mathbf{u}}}{\partial x^2} = \sum_{j=1}^N \alpha_j \frac{\partial^2 \phi_j}{\partial x^2}, \text{ etc} \quad (55)$$

**Table 1**  
[0°/90°] square laminated plate under zig-zag formulation.

$a/h$	Method	$\bar{w}$	$\bar{\sigma}_{xx}$	$\bar{\sigma}_{yy}$	$\bar{\tau}_{zx}$	$\bar{\tau}_{xy}$
4	HSDT (Reddy, 1984)	1.8937	0.6651	0.6322	0.2064	0.0440
	FSDT (Reddy and Chao, 1981)	1.7100	0.4059	0.5765	0.1398	0.0308
	Elasticity (Pagano, 1970) Present	1.954	0.720	0.666	0.270	0.0467
	(13 × 13grid)	1.8792	0.6348	0.7312	0.1977	0.0433
	Present (17 × 17grid)	1.8792	0.6348	0.7311	0.2052	0.0433
	Present (21 × 21grid)	1.8792	0.6348	0.7312	0.2088	0.0433
	Original Murakami (21 × 21grid)	1.8931	0.6408	0.8506	0.2160	0.0436
10	HSDT (Reddy, 1984)	0.7147	0.5456	0.3888	0.2640	0.0268
	FSDT (Reddy and Chao, 1981)	0.6628	0.4989	0.3615	0.1667	0.0241
	Elasticity (Pagano, 1970)	0.743	0.559	0.403	0.301	0.0276
	Present (13 × 13grid)	0.7291	0.5515	0.4116	0.2747	0.0272
	Present (17 × 17grid)	0.7291	0.5515	0.4117	0.2851	0.0272
	Present (21 × 21grid)	0.7291	0.5515	0.4117	0.2901	0.0272
	Original Murakami (21 × 21grid)	0.7227	0.5460	0.4194	0.2978	0.0269
100	HSDT (Reddy, 1984)	0.4343	0.5387	0.2708	0.2897	0.0213
	FSDT (Reddy and Chao, 1981)	0.4337	0.5382	0.2705	0.1780	0.0213
	Elasticity (Pagano, 1970) Present	0.4347	0.539	0.271	0.339	0.0214
	(13 × 13grid)	0.4355	0.5439	0.2744	0.3083	0.0214
	Present (17 × 17grid)	0.4356	0.5442	0.2739	0.3206	0.0214
	Present (21 × 21grid)	0.4357	0.5442	0.2738	0.3262	0.0214
	Original Murakami (21 × 21grid)	0.4294	0.5363	0.2699	0.3344	0.0211

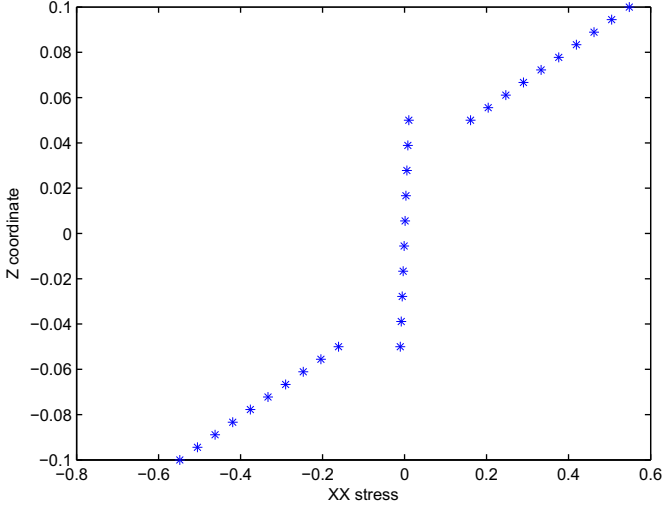


Fig. 4. Normalized normal  $\sigma_{xx}$  stress for  $a/h = 4$ ,  $21 \times 21$  points.

In the present collocation approach, we need to impose essential and natural boundary conditions. Consider, for example, the condition  $w=0$ , on a simply supported or clamped edge. We enforce the conditions by interpolating as

$$w = 0 \rightarrow \sum_{j=1}^N \alpha_j^w \phi_j = 0 \quad (56)$$

Other boundary conditions are interpolated in a similar way.

#### 4.7. Free vibrations problems

For free vibration problems we set the external force to zero, and assume harmonic solution in terms of displacements  $u_0, u_1, v_0, v_1, \dots$ , as

$$u_0 = U_0(w, y)e^{i\omega t}; \quad u_1 = U_1(w, y)e^{i\omega t}; \quad u_z = U_z(w, y)e^{i\omega t} \quad (57)$$

$$v_0 = V_0(w, y)e^{i\omega t}; \quad v_1 = V_1(w, y)e^{i\omega t}; \quad v_z = V_z(w, y)e^{i\omega t} \quad (58)$$

$$w_0 = W_0(w, y)e^{i\omega t}; \quad w_1 = W_1(w, y)e^{i\omega t}; \quad w_2 = W_2(w, y)e^{i\omega t} \quad (59)$$

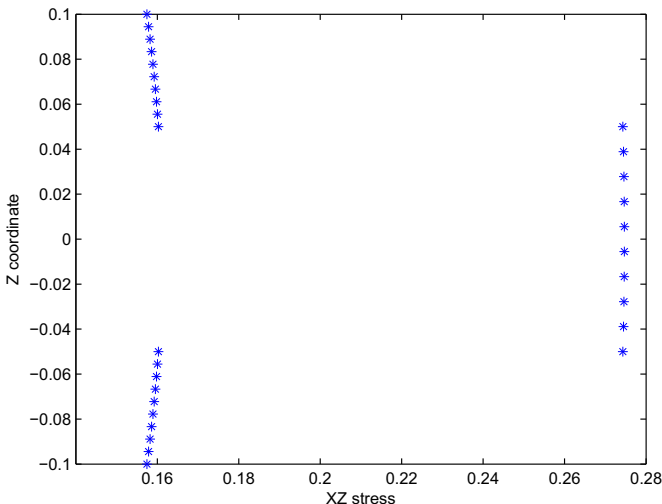


Fig. 5. Normalized transverse  $\tau_{xz}$  stress for  $a/h = 4$ ,  $21 \times 21$  points.

where  $\omega$  is the frequency of natural vibration. Substituting the harmonic expansion into Eqs. (52) in terms of the amplitudes  $U_0, U_1, U_z, V_0, V_1, V_z, W_0, W_1, W_2$ , we may obtain the natural frequencies and vibration modes for the plate problem, by solving the eigenproblem

$$[\mathcal{L} - \omega^2 \mathcal{G}] \mathbf{X} = 0 \quad (60)$$

where  $\mathcal{L}$  collects all stiffness terms and  $\mathcal{G}$  collects all terms related to the inertial terms. In (60)  $\mathbf{X}$  are the modes of vibration associated with the natural frequencies defined as  $\omega$ .

#### 4.8. Buckling analysis

The buckling analysis considers the addition into the equations of motion of terms  $\bar{N}_{xx} \partial^2 w / \partial x^2 + 2\bar{N}_{xy} \partial^2 w / \partial x \partial y + \bar{N}_{yy} \partial^2 w / \partial y^2$ , associated with equation in  $w_0$ , being  $\bar{N}_{xx}$ ,  $\bar{N}_{xy}$ , and  $\bar{N}_{yy}$  the in-plane applied forces. In order to determine the critical buckling load of the laminated plate, the transverse load and all inertial terms are set to zero.

The eigenproblem associated with the buckling problem is then defined as

$$[\mathcal{L} - \lambda \mathcal{G}] \mathbf{X} = 0 \quad (61)$$

where  $\mathcal{L}$  collects all stiffness terms and  $\mathcal{G}$  collects all terms related to the in-plane forces. In (63)  $\mathbf{X}$  are the buckling modes associated with the buckling loads defined as  $\lambda$ .

### 5. Numerical examples

All numerical examples consider a Chebyshev grid (illustrated in Fig. 3). the grid is generated by MATLAB code, for a given number of nodes per side ( $N$ ):

$$x = \cos(\pi * (0 : N) / N)';$$

$$y = x;$$

A Wendland function (Wendland, 1998) was used in all examples. This function is defined as

$$\phi(r) = (1 - cr)_+^8 (32(cr)^3 + 25(cr)^2 + 8cr + 1) \quad (62)$$

where the shape parameter ( $c$ ) was obtained by an optimization procedure, as detailed in Ferreira and Fasshauer (2006).

#### 5.1. Static problems-cross-ply laminated plates

A simply supported square laminated plate of side  $a$  and thickness  $h$  is composed of four equally layers oriented at  $[0^\circ/90^\circ]$ . The plate is subjected to a sinusoidal vertical pressure of the form

Table 2

The normalized fundamental frequency of the simply supported cross-ply laminated square plate  $[0^\circ/90^\circ]$  ( $\bar{\omega} = (\omega a^2 / h) \sqrt{\rho / E_2}$ ,  $h/a = 0.2$ ).

Method	Grid	$E_1/E_2$			
		10	20	30	40
Liew et al. (2003)		8.2924	9.5613	10.320	10.849
Exact (Reddy, 1997; Khdeir and Librescu, 1988)		8.2982	9.5671	10.326	10.854
Present zig-zag ( $\nu_{23} = 0.25$ )	$13 \times 13$	8.3325	9.6168	10.3708	10.8836
	$17 \times 17$	8.3324	9.6166	10.3707	10.8835
	$21 \times 21$	8.3324	9.6166	10.3707	10.8835



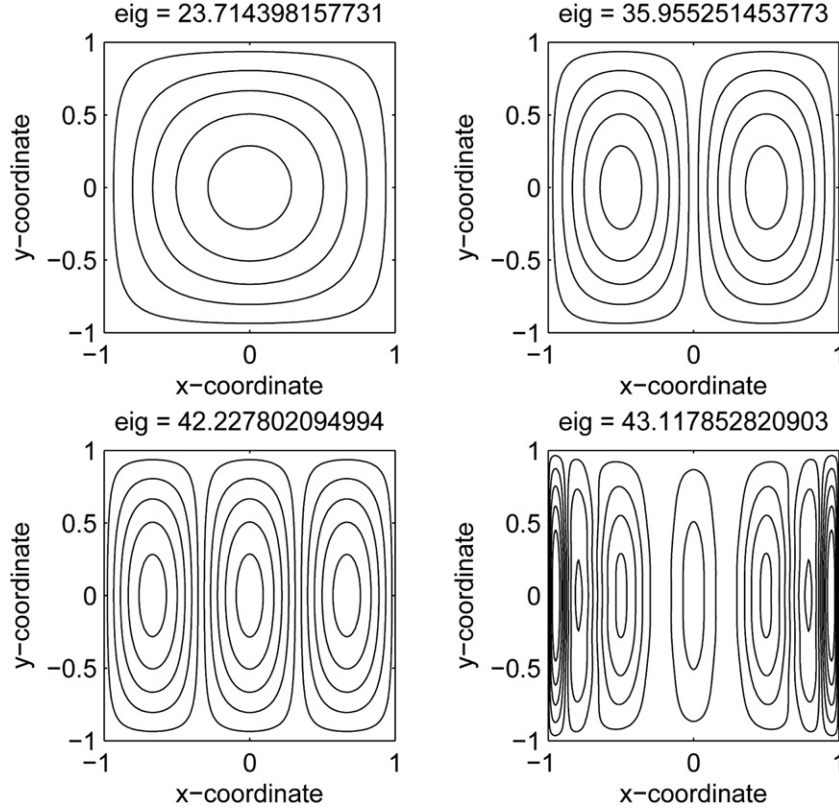


Fig. 6. First 4 buckling modes: Uni-axial buckling load of four-layer  $[0^\circ/90^\circ]$  simply supported laminated plate ( $\bar{N} = \bar{N}_{xx}a^2/(E_2h^3)$ ,  $\bar{N}_{xy} = 0$ ,  $\bar{N}_{yy} = 0$ ), grid  $13 \times 13$  points.

$$p_z = P \sin\left(\frac{\pi x}{a}\right) \sin\left(\frac{\pi y}{a}\right)$$

with the origin of the coordinate system located at the lower left corner on the midplane and  $P$  the maximum load (at center of plate).

The orthotropic material properties for each layer are given by

$$E_1 = 25.0E_2 \quad G_{12} = G_{13} = 0.5E_2 \quad G_{23} = 0.2E_2 \quad \nu_{12} = 0.25$$

The in-plane displacements, the transverse displacements, the normal stresses and the in-plane and transverse shear stresses are presented in normalized form as

$$\begin{aligned} \bar{w} &= \frac{10^2 w_{(a/2, a/2, 0)} h^3 E_2}{Pa^4} \quad \bar{\sigma}_{xx} = \frac{\sigma_{xx(a/2, a/2, h/2)} h^2}{Pa^2} \quad \bar{\sigma}_{yy} \\ &= \frac{\sigma_{yy(a/2, a/2, h/4)} h^2}{Pa^2} \quad \bar{\tau}_{xz} = \frac{\tau_{xz(0, a/2, 0)} h}{Pa} \quad \bar{\tau}_{xy} = \frac{\tau_{xy(0, 0, h/2, 0)} h^2}{Pa} \end{aligned}$$

In Table 1 we present results for the present ZZ theory, using  $11 \times 11$  up to  $21 \times 21$  points. We compare results with higher-order solutions by Akhras et al. (1994), and Reddy (1984), FSDT solutions

by Reddy and Chao (1981), and an exact solution by Pagano (1970). We also compare with results by the authors using RBFs with Reddy's theory (Ferreira et al., 2003), and a layerwise theory (Ferreira, 2005). Our ZZ theory produces excellent results, when compared with other HSDT theories, for all  $a/h$  ratios, for transverse displacements, normal stresses and transverse shear stresses. In Fig. 4 the  $\sigma_{xx}$  evolution across the thickness direction is illustrated, for  $a/h = 4$ , using  $21 \times 21$  points. In Fig. 5 the  $\tau_{xz}$  evolution across the thickness direction is illustrated, for  $a/h = 4$ , using  $21 \times 21$  points. Note that the transverse shear stresses are obtained directly from the constitutive equations. Results are compared with the original Murakami's displacement field. It can be concluded that the present formulation shows excellent accuracy with the original Murakami's approach.

## 5.2. Free vibration problems-cross-ply laminated plates

In this example, all layers of the laminate are assumed to be of the same thickness, density and made of the same linearly elastic composite material. The following material parameters of a layer are used:

Table 3

Uni-axial buckling load of four-layer  $[0^\circ/90^\circ]$  simply supported laminated plate ( $\bar{N} = \bar{N}_{xx}a^2/(E_2h^3)$ ,  $\bar{N}_{xy} = 0$ ,  $\bar{N}_{yy} = 0$ ).

Grid	Present	Liew and Huang (2003)	Khdeir and Librescu (1988)
Present- zig-zag			
$13 \times 13$	23.7144	23.463	23.453
$17 \times 17$	23.7135		
$21 \times 21$	23.7134		

Table 4

Bi-axial buckling load of three-layer  $[0^\circ/90^\circ]$  simply supported laminated plate ( $\bar{N} = \bar{N}_{xx}a^2/(E_2h^3)$ ,  $\bar{N}_{xy} = 0$ ,  $\bar{N}_{yy} = \bar{N}_{xx}$ ).

Grid	SS	SC	CC
Present – zig-zag			
$13 \times 13$	10.2100	11.7633	13.6591
$17 \times 17$	10.2089	11.7622	13.6582
$21 \times 21$	10.2088	11.7621	13.6581
Liew and Huang (2003)	10.178	11.575	13.260
Khdeir and Librescu (1988)	10.202	11.602	13.290

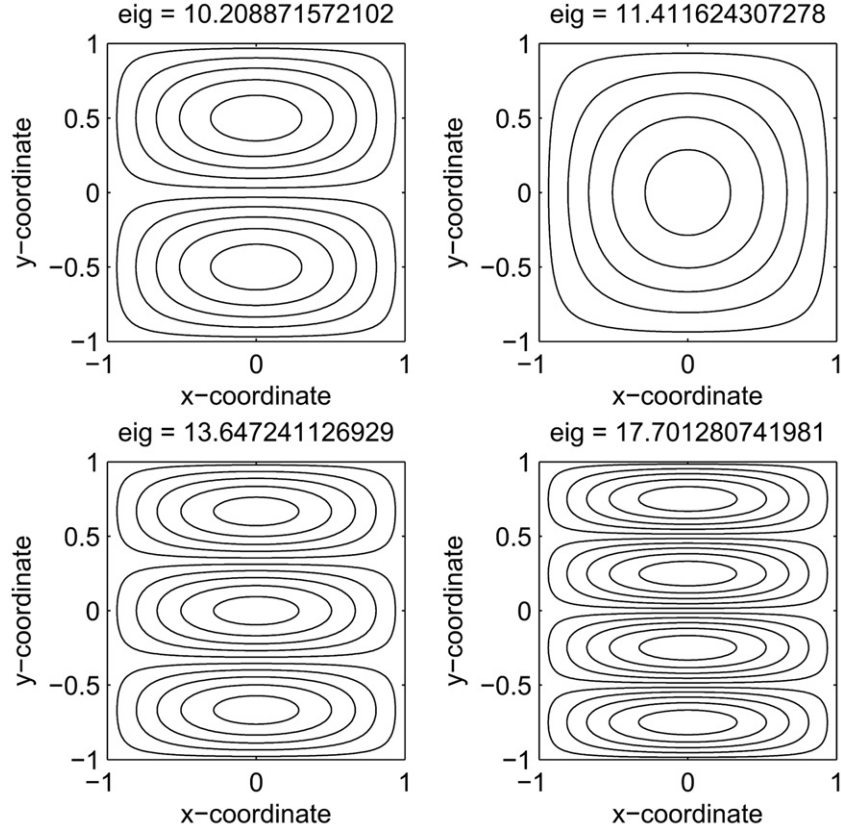


**Fig. 7.** First 4 buckling modes: Bi-axial buckling load of three-layer  $[0^\circ/90^\circ]$  simply supported (SSSS) laminated plate ( $\bar{N} = \bar{N}_{xx}a^2/(E_2h^3)$ ,  $\bar{N}_{xy} = 0$ ,  $\bar{N}_{yy} = \bar{N}_{xx}$ ), grid  $17 \times 17$  points.

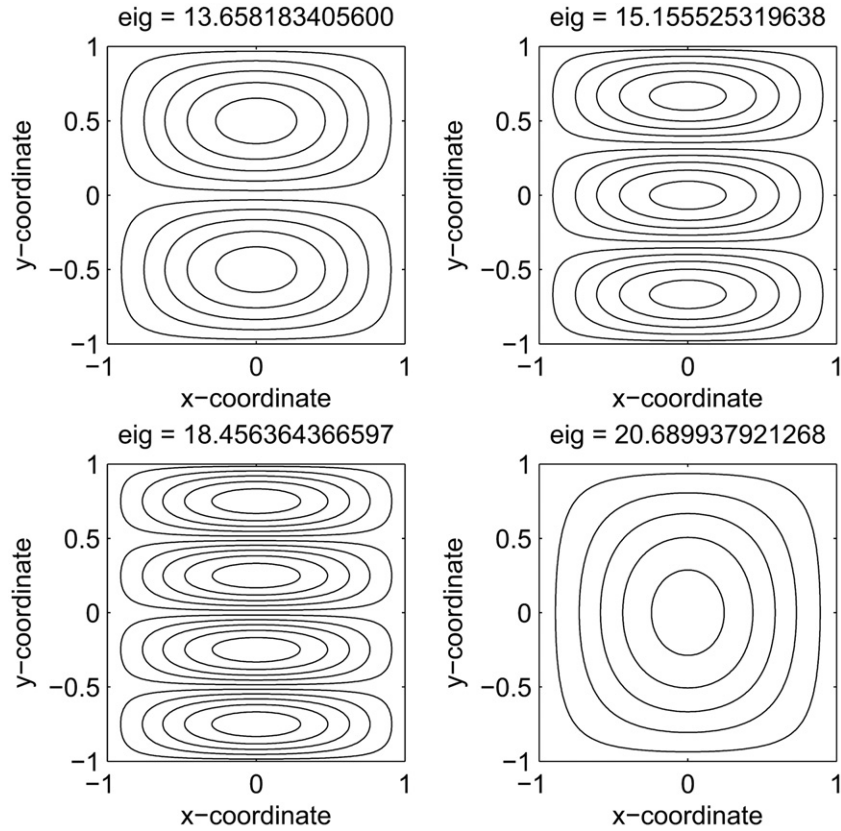


**Fig. 8.** First 4 buckling modes: Bi-axial buckling load of three-layer  $[0^\circ/90^\circ]$  SSSS laminated plate ( $\bar{N} = \bar{N}_{xx}a^2/(E_2h^3)$ ,  $\bar{N}_{xy} = 0$ ,  $\bar{N}_{yy} = \bar{N}_{xx}$ ), grid  $17 \times 17$  points.

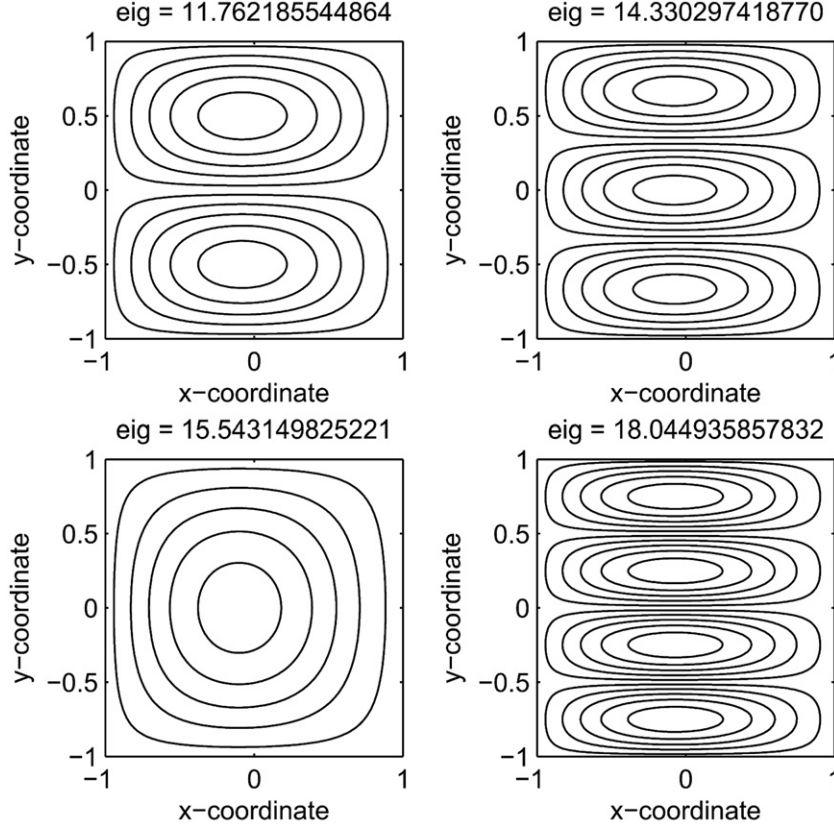


**Fig. 9.** First 4 buckling modes: Bi-axial buckling load of three-layer  $[0^\circ/90^\circ]$  SSSC laminated plate ( $\bar{N} = \bar{N}_{xx}a^2/(E_2h^3)$ ,  $\bar{N}_{xy} = 0$ ,  $\bar{N}_{yy} = \bar{N}_{xx}$ ), grid  $17 \times 17$  points.

$$\frac{E_1}{E_2} = 10, 20, 30 \text{ or } 40; G_{12} = G_{13} = 0.6E_2; G_3 = 0.5E_2; \nu_{12} = 0.25$$

The subscripts 1 and 2 denote the directions normal and transverse to the fiber direction in a lamina, which may be oriented at an angle to the plate axes. The ply angle of each layer is measured from the global  $x$ -axis to the fiber direction.

The example considered is a simply supported square plate of the cross-ply lamination  $[0^\circ/90^\circ]$ . The thickness and length of the plate are denoted by  $h$  and  $a$ , respectively. The thickness-to-span ratio  $h/a = 0.2$  is employed in the computation. Table 2 lists the fundamental frequency of the simply supported laminate made of various modulus ratios of  $E_1/E_2$ . It is found that the present meshless results are in very close agreement with the values of (Reddy, 1997; Khdeir and Librescu, 1988) and the mesh-free results of Liew et al. (2003) based on the FSDT.

### 5.3. Buckling examples

Three-layer  $[0^\circ/90^\circ]$  and four-layer  $[0^\circ/90^\circ/0^\circ]$  square cross-ply laminates are chosen to compute the uni- and bi-axial buckling loads (Fig. 6). The plate has width  $a$  and thickness  $h$ . The span-to-thickness ratio  $a/h$  is taken to be 10. All layers are assumed to be of the same thickness and material properties:

$$\begin{aligned} E_1/E_2 &= 40; G_{12}/E_2 = G_{13}/E_2 = 0.6; G_{23}/E_2 = 0.5; \nu_{12} \\ &= 0.25 \end{aligned}$$

Table 3 lists the uni-axial buckling loads of the four-layer simply supported laminated plate. Exact solutions by Khdeir and Librescu (1988) and differential quadrature results by Liew and Huang (2003) based on the FSDT are also presented for comparison. It is

found that the critical buckling load is obtained with a few grid points. The present results are in excellent correlation with those of Khdeir and Librescu (1988), and those of Liew and Huang (2003).

Table 4 tabulates the bi-axial buckling loads of the  $[0^\circ/90^\circ]$  laminated plate. The laminated plate is simply supported along the edges parallel to the  $x$ -axis while the other two edges may be simply supported (S), or clamped (C). The notations SS, SC, and CC refer to the boundary conditions of the two edges parallel to the  $x$ -axis only.

In Fig. 7 it is illustrated the first 4 buckling modes for bi-axial buckling load of three-layer  $[0^\circ/90^\circ]$  simply supported laminated plate ( $\bar{N} = \bar{N}_{xx}a^2/(E_2h^3)$ ,  $\bar{N}_{xy} = 0$ ,  $\bar{N}_{yy} = \bar{N}_{xx}$ ), using a grid of  $17 \times 17$  points.

In Fig. 8 it is illustrated the first 4 buckling modes for bi-axial buckling load of three-layer  $[0^\circ/90^\circ]$  SCSC laminated plate ( $\bar{N} = \bar{N}_{xx}a^2/(E_2h^3)$ ,  $\bar{N}_{xy} = 0$ ,  $\bar{N}_{yy} = \bar{N}_{xx}$ ), using a grid of  $17 \times 17$  points.

In Fig. 9 it is illustrated the first 4 buckling modes for bi-axial buckling load of three-layer  $[0^\circ/90^\circ]$  SSSC laminated plate ( $\bar{N} = \bar{N}_{xx}a^2/(E_2h^3)$ ,  $\bar{N}_{xy} = 0$ ,  $\bar{N}_{yy} = \bar{N}_{xx}$ ), using a grid of  $17 \times 17$  points.

It is found that excellent agreement is achieved for all edge conditions considered when comparing the results obtained by the present radial basis function approach with the FSDT solutions by Khdeir and Librescu (1988), and those of Liew and Huang (2003), who use a MLS/DQ approach. Note that although comparison with other sources are excellent, the critical loads are related to the second mode (SSSS), fourth mode (SCSC) and third mode (SSSC).

## 6. Conclusions

In this paper we presented a study using the radial basis function collocation method to analyse static deformations, free vibrations and buckling loads of thin and thick laminated plates using

a variation of Murakami's zig-zag function, allowing for through-the-thickness deformations. This has not been done before and serves to fill the gap of knowledge in this area.

Using the Unified Formulation with the radial basis collocation, all the  $C^0$  plate formulations can be easily discretized by radial basis functions collocation. Also, the burden of deriving the equations of motion and boundary conditions is eliminated with the present approach. All is needed is to change one vector  $F_t$  that defines the expansion of displacements.

We analysed square cross-ply laminated plates in bending, free vibrations and buckling loads. The present results were compared with existing analytical solutions or competitive finite element solutions and excellent agreement was observed in all cases.

The present method is a simple yet powerful alternative to other finite element or meshless methods in the static deformation and free vibration analysis of thin and thick isotropic or laminated plates.

## Acknowledgement

The support of Ministério da Ciência Tecnologia e do Ensino superior and Fundo Social Europeu (MCTES and FSE) under programs POPH-QREN are gratefully acknowledged.

## References

- Akhraş, G., Cheung, M.S., Li, W., 1994. Finite strip analysis for anisotropic laminated composite plates using higher-order deformation theory. *Computers & Structures* 52 (3), 471–477.
- Altenbach, H., 1998. Theories for laminated and sandwich plates. a review. *International Applied Mechanics* 34, 243–252.
- Brischetto, S., Carrera, E., Demasi, L., 2009. Improved bending analysis of sandwich plate by using zig-zag function. *Computers & Structures* 89, 408–415.
- Burton, S., Noor, A.K., 1995. Assessment of computational model for sandwich panels and shells. *Computer Methods in Applied Mechanics and Engineering* 124, 125–151.
- Carrera, E., Kroplin, B., 1997. Zig-zag and interlaminar equilibria effects in large deflection and post-buckling analysis of multilayered plates. *Mechanics of Composite Materials and Structures* 4, 69–94.
- Carrera, E., 1996. C0 reissner-mindlin multilayered plate elements including zig-zag and interlaminar stress continuity. *International Journal of Numerical Methods in Engineering* 39, 1797–1820.
- Carrera, E., 1998. Evaluation of layer-wise mixed theories for laminated plate analysis. *AIAA Journal* 36, 830–839.
- Carrera, E., 2001. Developments, ideas, and evaluations based upon reissner's mixed variational theorem in the modelling of multilayered plates and shells. *Applied Mechanics Reviews* 54, 301–329.
- Carrera, E., 2003. Historical review of zig-zag theories for multilayered plates and shells. *Applied Mechanics Reviews* 56, 287–308.
- Carrera, E., 2004. The use of murakami's zig-zag function in the modeling of layered plates and shells. *Computers & Structures* 82, 541–554.
- Chen, X.L., Liu, G.R., Lim, S.P., 2003. An element free galerkin method for the free vibration analysis of composite laminates of complicated shape. *Composite Structures* 59, 279–289.
- Dai, K.Y., Liu, G.R., Lim, S.P., Chen, X.L., 2004. An element free galerkin method for static and free vibration analysis of shear-deformable laminated composite plates. *Journal of Sound and Vibration* 269, 633–652.
- Demasi, L., 2008a. 2d, quasi 3d and 3d exact solutions for bending of thick and thin sandwich plates. *Journal of Sandwich Structures and Materials* 10, 271–310.
- Demasi, L., 2008b.  $\infty^3$  hierarchy plate theories for thick and thin composite plates: the generalized unified formulation. *Computers & Structures* 84, 256–270.
- Ferreira, A.J.M., Fasshauer, G.E., 2006. Computation of natural frequencies of shear deformable beams and plates by a rbf-pseudospectral method. *Computer Methods in Applied Mechanics and Engineering* 196, 134–146.
- Ferreira, A.J.M., Roque, C.M.C., Martins, P.A.L.S., 2003. Analysis of composite plates using higher-order shear deformation theory and a finite point formulation based on the multiquadric radial basis function method. *Composites: Part B* 34, 627–636.
- Ferreira, A.J.M., 2003a. A formulation of the multiquadric radial basis function method for the analysis of laminated composite plates. *Composite Structures* 59, 385–392.
- Ferreira, A.J.M., 2003b. Thick composite beam analysis using a global meshless approximation based on radial basis functions. *Mechanics of Advanced Materials and Structures* 10, 271–284.
- Ferreira, A.J.M., 2005. Analysis of composite plates using a layerwise deformation theory and multiquadrics discretization. *Mechanics of Advanced Materials and Structures* 12 (2), 99–112.
- Hardy, R.L., 1971. Multiquadric equations of topography and other irregular surfaces. *Geophysical Research* 76, 1905–1915.
- Huang, Y.Q., Li, Q.S., 2004. Bending and buckling analysis of antisymmetric laminates using the moving least square differential quadrature method. *Computer Methods in Applied Mechanics and Engineering* 193, 3471–3492.
- Hon, Y.C., Lu, M.W., Xue, W.M., Zhu, Y.M., 1997. Multiquadric method for the numerical solution of bi-phase mixture model. *Applied Mathematics and Computation* 88, 153–175.
- Hon, Y.C., Cheung, K.F., Mao, X.Z., Kansa, E.J., 1999. A multiquadric solution for the shallow water equation. *ASCE Journal of Hydraulic Engineering* 125 (5), 524–533.
- Kansa, E.J., 1990. Multiquadrics- a scattered data approximation scheme with applications to computational fluid dynamics. I: surface approximations and partial derivative estimates. *Computers and Mathematics with Applications* 19 (8/9), 127–145.
- Khdeir, A.A., Librescu, L., 1988. Analysis of symmetric cross-ply elastic plates using a higher-order theory, part ii: buckling and free vibration. *Composite Structures* 9, 259–277.
- Kirchhoff, G., 1850. Über das gleichgewicht und die bewegung einer elastischen scheibe. *Journal für reine und angewandte Mathematik* 40, 51–88.
- Librescu, L., Hase, T., 2000. Recent developments in the modeling and behaviors of advanced sandwich constructions: a survey. *Computers & Structures* 48, 1–17.
- Liew, K.M., Huang, Y.Q., 2003. Bending and buckling of thick symmetric rectangular laminates using the moving least-squares differential quadrature method. *International Journal of Mechanical Science* 45, 95–114.
- Liew, K.M., Huang, Y.Q., Reddy, J.N., 2003. Vibration analysis of symmetrically laminated plates based on fsdt using the moving least squares differential quadrature method. *Computer Methods in Applied Mechanics and Engineering* 192, 2203–2222.
- Liew, K.M., Chen, X.L., Reddy, J.N., 2004. Mesh-free radial basis function method for buckling analysis of non-uniformity loaded arbitrarily shaped shear deformable plates. *Computer Methods in Applied Mechanics and Engineering* 193, 205–225.
- Liu, G.R., Chen, X.L., 2002. Buckling of symmetrically laminated composite plates using the element-free galerkin method. *International Journal of Structural Stability and Dynamics* 2, 281–294.
- Liu, G.R., Gu, Y.T., 2001. A local radial point interpolation method (lrpim) for free vibration analyses of 2-d solids. *Journal of Sound and Vibration* 246 (1), 29–46.
- Liu, G.R., Nguyen Thoi, Trung, 2010. *Smoothed Finite Element Method*. CRC Press, Boca Raton, USA.
- Liu, G.R., Wang, J.G., 2002. A point interpolation meshless method based on radial basis functions. *International Journal for Numerical Methods in Engineering* 54, 1623–1648.
- Liu, L., Liu, G.R., Tan, V.C.B., 2002. Element free method for static and free vibration analysis of spatial thin shell structures. *Computer Methods in Applied Mechanics and Engineering* 191, 5923–5942.
- Liu, G.R., Nguyen-Thoi, T., Lam, K.Y., 2009. An edge-based smoothed finite element method (es-fem) for static, free and forced vibration analyses in solids. *Journal of Sound and Vibration* 320, 1100–1130.
- Mindlin, R.D., 1951. Influence of rotary inertia and shear in flexural motions of isotropic elastic plates. *Journal of Applied Mechanics* 18, 31–38.
- Murakami, H., 1986. Laminated composite plate theory with improved in-plane responses. *Journal of Applied Mechanics* 53, 661–666.
- Nguyen-Thoi, T., Liu, G.R., Vu-Do, H.C., Nguyen-Xuan, H., 2009. An edge-based smoothed finite element method (es-fem) for visco-elastoplastic analyses of 2d solids using triangular mesh. *Computational Mechanics* 45, 23–44.
- Nguyen-Thoi, T., Liu, G.R., Nguyen-Xuan, H., 2010. An n-sided polygonal edge-based smoothed finite element method (nes-fem) for solid mechanics. *International Journal for Numerical Methods in Biomedical Engineering*. doi:10.1002/cnm.1375.
- Nguyen-Xuan, H., Liu, G.R., Thai-Hoang, C., Nguyen-Thoi, T., 2009a. An edge-based smoothed finite element method with stabilized discrete shear gap technique for analysis of reissner-mindlin plates. *Computer Methods in Applied Mechanics and Engineering* 199, 471–489.
- Nguyen-Xuan, H., Liu, G.R., Nguyen-Thoi, T., Nguyen-Tran, C., 2009b. An edge-based smoothed finite element method for analysis of two-dimensional piezoelectric structures. *Smart Materials and Structures* 18 (6), 065015.
- Noor, A.K., Burton, S., Bert, C.W., 1996. Computational model for sandwich panels and shells. *Applied Mechanical Reviews* 49, 155–199.
- Pagano, N.J., 1970. Exact solutions for rectangular bidirectional composites and sandwich plates. *Journal of Composite Materials* 4, 20–34.
- Reddy, J.N., Chao, W.C., 1981. A comparison of closed-form and finite-element solutions of thick laminated anisotropic rectangular plates. *Nuclear Engineering and Design* 64, 153–167.
- Reddy, J.N., 1984. A simple higher-order theory for laminated composite plates. *Journal of Applied Mechanics* 51, 745–752.
- Reddy, J.N., 1997. *Mechanics of Laminated Composite Plates: Theory and Analysis*. CRC Press, Boca Raton.
- Reissner, E., 1945. The effect of transverse shear deformations on the bending of elastic plates. *Journal of Applied Mechanics* 12, A69–A77.
- Vinson, J.R., 1999. *The Behavior of Sandwich Structures of Isotropic and Composite Materials*. Technomic Publishing Co.
- Vinson, J.R., 2001. Sandwich structures. *Applied Mechanical Reviews* 54, 201–214.
- Wang, J.G., Liu, G.R., 2002. On the optimal shape parameters of radial basis functions used for 2-d meshless methods. *Computer Methods in Applied Mechanics and Engineering* 191, 2611–2630.

- Wang, J.G., Liu, G.R., Lin, P., 2002. Numerical analysis of biot's consolidation process by radial point interpolation method. *International Journal of Solids and Structures* 39 (6), 1557–1573.
- Wen, P.H., Hon, Y.C., 2007. Geometrically nonlinear analysis of reissner-mindlin plates by meshless computation. *Computer Modelling in Engineering and Sciences* 21 (3), 177–254.
- Wendland, H., 1998. Error estimates for interpolation by compactly supported radial basis functions of minimal degree. *Journal of Approximation Theory* 93, 258–296.
- Xiang, S., Wang, K.M., Ai, Y.T., Sha, Y.D., Shi, H., 2009. Analysis of isotropic, sandwich and laminated plates by a meshless method and various shear deformation theories. *Composite Structures* 91 (1), 31–37.
- Xiang, S., Shi, H., Wang, K.M., Ai, Y.T., Sha, Y.D., 2010. Thin plate spline radial basis functions for vibration analysis of clamped laminated composite plates. *European Journal of Mechanics A/Solids* 29, 844–850.
- Zenkert, D., 1995. *An Introduction to Sandwich Structures*. Chamelon Press, Oxford.